

1 Modern and Reproducible Groundwater Modeling Workflows with  
2 FloPy

3 Joseph D. Hughes<sup>1</sup>, Christian D. Langevin<sup>2</sup>, Scott R. Paulinski<sup>3</sup>, Joshua D. Larsen<sup>4</sup>, and  
4 David Brakenhoff<sup>5</sup>

5 <sup>1</sup>U.S. Geological Survey, Model Support and Maintenance Branch, 927 W Belle Plaine Ave,  
6 Chicago, IL, USA

7 <sup>2</sup>U.S. Geological Survey, Model Support and Maintenance Branch, 2280 Woodale Dr, Mounds  
8 View, MN, USA

9 <sup>3</sup>U.S. Geological Survey, California Water Science Center, 4165 Spruance Road, Suite 200, San  
10 Diego, CA, USA

11 <sup>4</sup>U.S. Geological Survey, California Water Science Center, 6000 J Street, Placer Hall,  
12 Sacramento, CA, USA

13 <sup>5</sup>Artesia Water, Korte Weistraat 12, Schoonhoven, Netherlands

14 November 16, 2022

15 **Abstract**

16 FloPy functionality has been expanded from the capabilities described in Bakker et al. (2016) to  
17 support the latest version of MODFLOW (MODFLOW 6). FloPy classes are automatically generated  
18 using the same files used to generate the MODFLOW 6 input guide, which allows new features  
19 to be supported immediately and FloPy to be a critical component for MODFLOW 6 development  
20 and testing. FloPy can be used to download MODFLOW-based and other executables for Linux,  
21 Mac OS, and Windows operating systems, which simplifies the process required to download and use  
22 these executables. Expanded FloPy capabilities include (1) full support for structured (DIS), layer-  
23 based unstructured (DISV), and fully-unstructured (DISU) MODFLOW 6 discretization types; (2)  
24 geoprocessing of shapefile-like and raster data to develop model data for all MODFLOW 6 discretization  
25 types; (3) the addition of functionality to provide user-centric access to simulated output data;  
26 (4) extension of plotting capabilities to unstructured MODFLOW 6 discretization types; and (5)  
27 the ability to export model, package, and individual array data to shapefiles, NetCDF, and VTK  
28 formats for processing, analysis, and visualization by other software products. Examples of using  
29 expanded FloPy capabilities are presented for a hypothetical watershed. An unstructured ground-  
30 water flow and transport model, with several advanced stress packages, is presented to demonstrate  
31 how FloPy can be used to develop complicated model datasets from original source data (shapefiles  
32 and rasters), post-process model results, and plot simulated results.

33 **1 Introduction**

34 FloPy is a popular Python package for constructing, running, and post processing MODFLOW-based  
35 groundwater flow and transport models (Bakker et al. 2016). It is an open-source Python package  
36 developed by a growing community of contributors. The combination of open-source programming  
37 languages (such as Python) with version control software (such as Git) allow the model construction  
38 process to be documented, reproducible and easily inspected and used by others. This workflow has

been recommended as one way to facilitate repeatable research and sharing of ideas (Fienen and Bakker 2016). Bakker et al. (2016) describe the general approach for working with models within the Python environment and emphasize the reproducible nature of developing models through scripting.

FloPy has been used to pioneer new methods and analysis tools, such as deep learning approaches for improving groundwater model calibration (Sun 2018; Zhou and Tartakovsky 2021), regionalizing residence times using metamodeling (Starn and Belitz 2018), applying iterative ensemble approaches for calibration and uncertainty quantification (White 2018), and exploring alternative parameterization schemes for risk analysis (Knowling et al. 2019). There are numerous examples of constructing MODFLOW models with FloPy to solve applied groundwater problems (Befus et al. 2017; van Engelen et al. 2018; Ebeling et al. 2019; Zipper et al. 2019; Befus et al. 2020). FloPy is used in GIS-based tools, such as FREEWAT (Rossetto et al. 2018) and other cyberinfrastructures (Essawy et al. 2018) to export models into MODFLOW datasets. FloPy can also be used as the “glue” to help couple MODFLOW to other hydrological models (Burek et al. 2020) or, for example, to agent-based models designed to quantify the effects of decision makers on environmental behavior (Jaxa-Rozen et al. 2019).

We use FloPy extensively to teach MODFLOW and groundwater modeling to early- and mid-career engineers and scientists. Other organizations also use FloPy to teach MODFLOW (for example, Hatari Labs and the Australian Water School). Annotated Jupyter notebooks and example scripts are useful demonstrating concepts and provide a resource that can be used as templates for developing real-world model applications. We routinely rely on FloPy to load and help identify problems in user model applications, and with the initial release of the MODFLOW 6 groundwater flow model (Langevin et al. 2017), we started to rely on FloPy to help with development of the MODFLOW program. We write tests that rely on FloPy to construct and run models, and then read output. We then verify that the output is as expected, by using analytical solutions, other models, or results that have been confirmed to be correct.

The purpose of this paper is to highlight important FloPy advances since it was first described by Bakker et al. (2016), provide examples that demonstrate these new capabilities, and reinforce the advantages of the modern scripting workflow for developing reproducible groundwater flow and transport models that can be easily updated as new data become available. The important advances described here include (1) complete support for all models, packages, and options implemented in the core version of MODFLOW supported by the U.S. Geological Survey (Hughes et al. 2017; Langevin et al. 2017; Provost et al. 2017; Langevin et al. 2020; Morway et al. 2021; Langevin et al. 2022; Hughes et al. 2022; Mancewicz et al. 2022); (2) generalized support for models based on a regular grid consisting of layers, rows, and columns, and also for models based on unstructured grids; (3) implementation of new geoprocessing capabilities to rapidly populate models with data from a variety of input sources; (4) simplified access to model results; (5) plotting capabilities for map and cross-section views of model data; and (6) export capabilities for writing model data to a variety of output formats.

## 2 FloPy Support for MODFLOW 6

The most recent version of MODFLOW (MODFLOW 6) is an object-oriented program and framework developed to provide a platform for supporting multiple models and multiple types of models within the same simulation (Hughes et al. 2017). These models can be independent of one another with no interaction, they can exchange coefficients and dependent variables (for example, head), or they can be tightly coupled at the matrix level by adding them to the same numerical solution. Transfer of information between models is isolated to exchange objects, which allow models to be developed and used independently. Within this new framework, a regional-scale groundwater model may be coupled with multiple local-scale groundwater models.

MODFLOW 6 currently includes the Groundwater Flow (GWF) Model and the Groundwater

85 Transport (GWT) Model each with packages to represent surface water processes, groundwater ex-  
86 traction, external boundaries, mass sources and sinks, and mass sorption and reactions. GWF and  
87 GWT models can be developed using regular model grids consisting of layers, rows, and columns or  
88 they can be developed using more general unstructured grids using many of the concepts and numerical  
89 approaches available in MODFLOW-USG ([Panday et al. 2013](#)). MODFLOW 6 also includes advanced  
90 formulations to simulate three-dimensional anisotropy and dispersion ([Provost et al. 2017](#)), coupled  
91 variable-density groundwater flow and transport ([Langevin et al. 2020](#)), and a water mover package to  
92 represent natural and managed hydrologic connections ([Morway et al. 2021](#)).

93 Development and testing of the MODFLOW 6 program relies heavily on tight integration with  
94 FloPy. A key component of this tight integration is the capability to quickly support new MODFLOW  
95 6 models and packages with FloPy. Unlike the FloPy support for previous MODFLOW versions (for  
96 example, MODFLOW-2005, MODFLOW-NWT, MODFLOW-USG, and SEAWAT), the FloPy Python  
97 classes for MODFLOW 6 are dynamically generated from simple text files, called “definition files,” that  
98 describe the input file structure (Figure 1). All MODFLOW 6 model input files are described using  
99 these definition files. This allows MODFLOW 6 developers to write tests for new models, packages,  
100 and functionality as they are developed. These definition files are used to generate the user input  
101 and output guide. These same definition files are also used to generate FloPy classes, with argument  
102 **docstrings** corresponding to input variable descriptions in the input and output guide. Definition  
103 files used to create FloPy Python classes for MODFLOW 6 are located in the `flopymf6/data/dfn/`  
104 subdirectory **in the site-packages directory for a Python distribution or Python environment**. The  
105 FloPy Python classes for MODFLOW 6 can be regenerated using

```
106 >>> import flopymf6
107 >>> flopymf6.utils.createpackages.create_packages()
```

108 New functionality can be added by users to existing packages by modifying existing definition files  
109 using instructions provided in the [MODFLOW 6 GitHub repository](#). The existing definition files  
110 can also be used as a template for creating classes for new MODFLOW 6 models or packages.  
111 New definition files should be placed in the `flopymf6/data/dfn/` subdirectory prior to rerunning  
112 `flopymf6.utils.createpackages.create_packages()`.

### 113 3 Common Modeling Tasks

#### 114 3.1 Getting MODFLOW and Other Related Executables

115 FloPy for MODFLOW 6 relies on a number of helper classes, which wrap functionality available in  
116 pre-compiled external executables, to generate unstructured models and calculate water budgets on  
117 user-defined zones. To facilitate getting these executables and other MODFLOW and related programs  
118 (for example, MODPATH, MT3DMS, MT3D-USGS, SEAWAT, etc.) can be installed using

```
119 get-modflow :flopymf6
```

120 in a terminal or at the command line after installing FloPy. The `get-modflow` command downloads  
121 the latest release of MODFLOW and related programs for the operating system the command is run  
122 on (Windows, MacOS, or Linux) from an [Executables GitHub repository](#). `get-modflow` can also  
123 download previous versions of MODFLOW 6 and the latest development version of MODFLOW 6  
124 using instructions available on the [FloPy GitHub repository](#).

## MODFLOW 6 Input and Output Guide

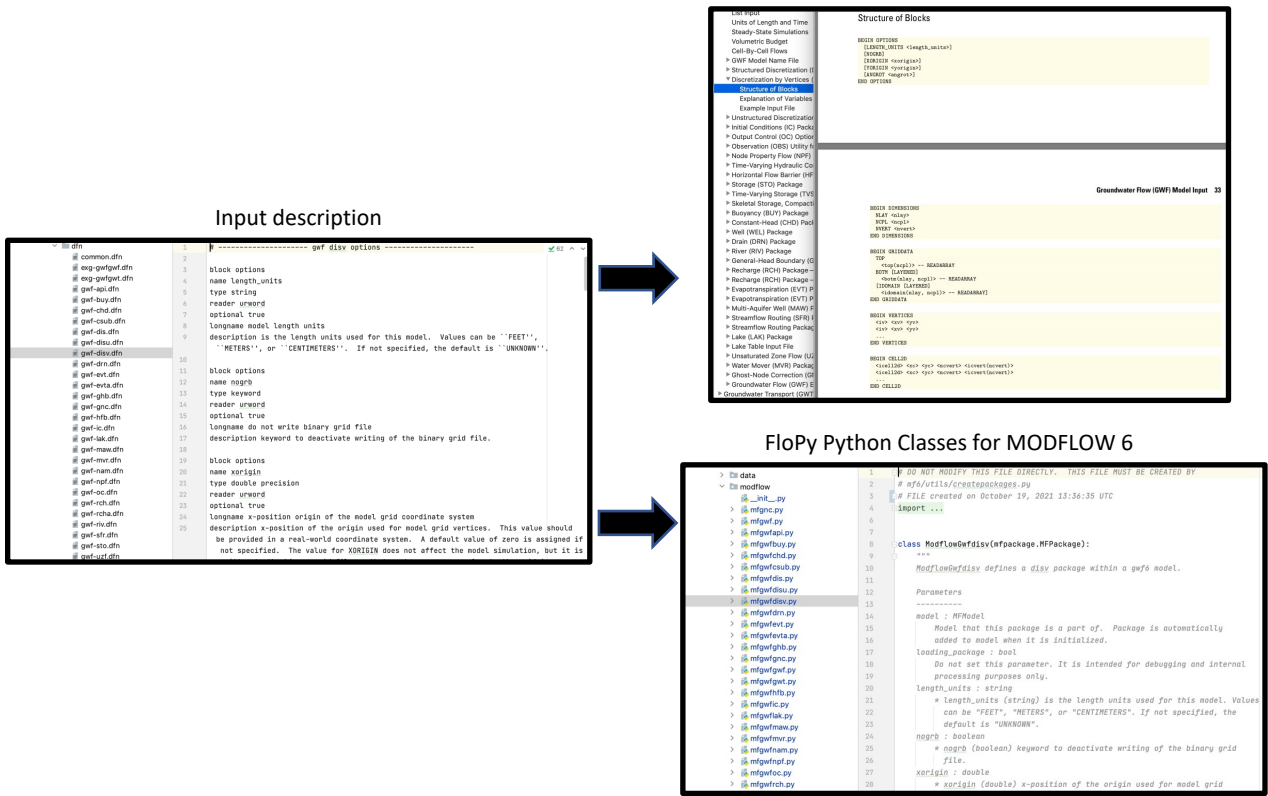


**Figure 1:** Relation between MODFLOW 6 input description files and the MODFLOW 6 input and output guide and the FloPy Python classes for MODFLOW 6.

### 125 3.2 Managing and Creating Model Grids

126 FloPy was originally developed to support models that are based on a regular grid consisting of lay-  
 127 ers, rows, and columns. With recent support for unstructured grids in MODFLOW (Panday et al.  
 128 2013; Langevin et al. 2017) it became necessary to revise the underlying approach for managing spa-  
 129 tial discretization information in FloPy. The goal was to containerize grid information into a single  
 130 location and use this information throughout FloPy modeling tasks for geospatial processing, plot-  
 131 ting, and exporting. Spatial discretization is now handled in FloPy through dedicated model grid  
 132 classes. There is a `Grid` class, which serves as the base class for the `StructuredGrid`, `VertexGrid`,  
 133 and `UnstructuredGrid` classes. Grid objects can be created by the user for preprocessing, and they  
 134 will be automatically generated and attached to a FloPy model object.

135 Regular MODFLOW grids can have constant row and column spacings, as shown in Figure 2A, or  
 136 they can have variable row and column spacings to focus resolution around an area of interest, as shown  
 137 in Figure 2B. The following Python code shows how to create a `StructuredGrid` object in FloPy. A  
 138 `StructuredGrid` object will also be created from discretization data required when instantiating a  
 139 MODFLOW 6 DIS object using `flopyp.mf6.ModflowGwfdis()`.

```
140 >>> regular_grid = flopyp.discretization.StructuredGrid(nlay=nlay,
141 ... delr=delr, delc=delc, xoff=0.0, yoff=0.0, angrot=0.0, top=top, botm=botm)
```

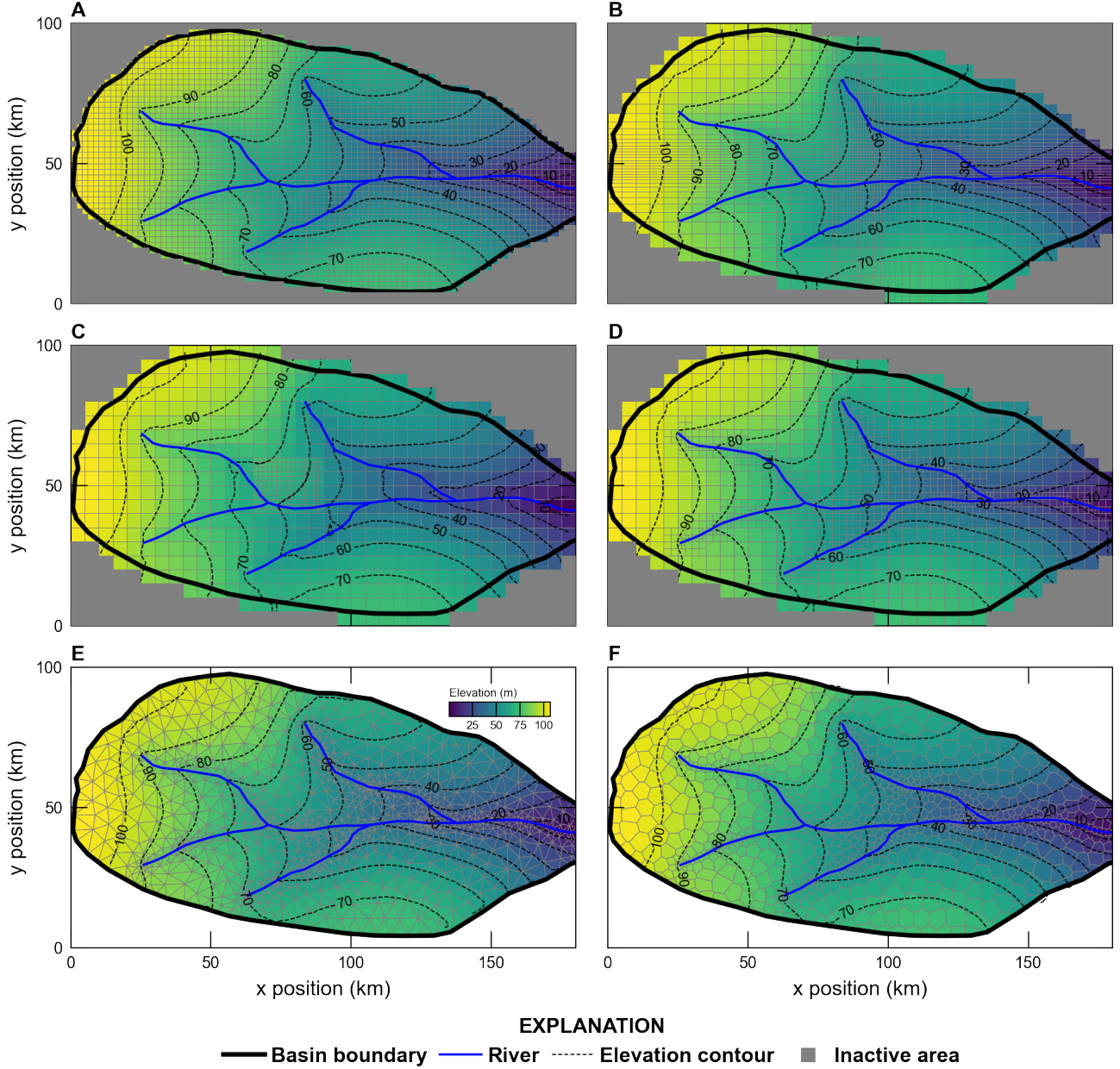


Figure 2: Examples of grids that can be generated and processed using FloPy for a hypothetical watershed, including (A) a regular MODFLOW grid with constant and equal row and column spacings, (B) a regular MODFLOW grid with variable row and column spacings, (C) a regular MODFLOW child grid nested within a regular MODFLOW parent grid, (D) a quadtree grid generated with the GRIDGEN program (Lien et al. 2014) through the FloPy wrapper, (E) a triangular grid generated with the Triangle program (Shewchuk 1996) through the FloPy wrapper, and (F) a Voronoi grid created from the triangular mesh.

142 MODFLOW 6 was developed to natively support multi-model simulations (Hughes et al. 2017).  
 143 One form of multi-model simulation is a nested grid application in which a more finely discretized child  
 144 model is embedded within a more coarsely discretized parent model (Mehl and Hill 2006; Vilhelmsen  
 145 et al. 2012; Mehl and Hill 2013). The use of a locally refined grid (LGR) within a parent grid offers

146 computation benefits in that the additional refinement is targeted to an area of interest. FloPy provides  
 147 a utility class, called `Lgr()` for constructing the data required to tightly couple parent and child models  
 148 within a single MODFLOW 6 simulation. Figure 2C shows two `StructuredGrid` objects—one object  
 149 represents the parent model grid and the other represents the nested child grid. The `Lgr()` class defines  
 150 the connection properties between cells in the parent model and cells in the child model. The utility  
 151 is general in that the child model can have more layers than the parent model.

152 FloPy supports management and generation of unstructured grids. Unstructured grids are rep-  
 153 resented in FloPy as being layered or fully unstructured. A layered grid is one in which the same  
 154 grid applies to all model layers. An unstructured grid is more general and allows the model grid to  
 155 change with depth. Layered grids and unstructured grids are stored in FloPy as `VertexGrid` and  
 156 `UnstructuredGrid` objects, respectively.

157 A layered quadtree grid can be created with FloPy using the `Gridgen()` utility class, which is a  
 158 wrapper around the GRIDGEN program (Lien et al. 2014). GRIDGEN starts with a regular MOD-  
 159 FLOW grid provided by the user. The program then recursively subdivides individual cells that  
 160 intersect with refinement features into quarters until a maximum level of refinement is met. Refine-  
 161 ment features may be points, lines, or polygons. Smoothing is automatically handled so that a cell is  
 162 connected to no more than two cells in any primary horizontal direction and four cells in the vertical  
 163 direction. Figure 2D shows an example of a quadtree grid created with GRIDGEN in which a base  
 164 grid is refined along streams. The following Python code shows the steps for creating the quadtree  
 165 grid with GRIDGEN.

```
166 >>> sim = flopy.mf6.MFSimulation()
167 >>> gwf = flopy.mf6.ModflowGwf(sim)
168 >>> dis6 = flopy.mf6.ModflowGwfdis(gwf, nrow=nrow, ncol=ncol, delr=dy, delc=dx)
169 >>> g = Gridgen(dis6, model_ws=temp_path)
170 >>> g.add_refinement_features([[closed_polygon]], "polygon", 0, range(1))
171 >>> g.add_refinement_features(stream_points, "line", 2, range(1))
172 >>> g.build(verbose=False)
173 >>> gridprops_vg = g.get_gridprops_vertexgrid()
174 >>> quadtree_grid = flopy.discretization.VertexGrid(**gridprops_vg)
```

175 FloPy also provides a wrapper utility for the Triangle mesh generation program (Shewchuk 1996).  
 176 The FloPy (`Triangle()`) utility class writes the Triangle program input file, runs the Triangle program,  
 177 and then loads the triangular mesh. Users provide the maximum area for individual triangles, angle  
 178 constraints, a polygon describing the model domain, and so forth. Figure 2E shows an example of a  
 179 triangular grid created with the Triangle program. The Python code for creating the triangular grid  
 180 is shown below.

```
181 >>> tri = flopy.utils.triangle.Triangle(maximum_area=maximum_area,
182 ... angle=30, nodes=nodes, model_ws=temp_path)
183 ...
184 >>> tri.add_polygon(boundary_points)
185 >>> tri.build(verbose=False)
186 >>> cell2d = tri.get_cell2d()
187 >>> vertices = tri.get_vertices()
188 >>> triangular_grid = VertexGrid(vertices=vertices, cell2d=cell2d,
189 ... idomain=idomain, nlay=nlay, ncpl=tri.ncpl, top=top, botm=botm)
```

191 A triangular grid can be converted into a Voronoi grid using the `VoronoiGrid()` utility class within  
 192 FloPy. This utility class uses SciPy routines ([Virtanen et al. 2020](#)) to construct Voronoi polygons  
 193 around each vertex in the triangular mesh. Figure 2F shows an example of a Voronoi grid created from  
 194 the triangular mesh shown in Figure 2D. The steps for creating the Voronoi grid from the `Triangle`  
 195 object are shown below.

```
196 >>> vor = flopy.utils.voronoi.VoronoiGrid(tri)
197 >>> gridprops = vor.get_gridprops_vertexgrid()
198 >>> voronoi_grid = VertexGrid(**gridprops, nlay=nlay, idomain=idomain)

199 StructuredGrid, VertexGrid, and UnstructuredGrid grid objects have useful properties (.property)
200 and methods (.method()) for accessing or mapping locations on the model grid including: (1) con-
201 version of xy pairs from local to global coordinates (.get_coords()) and from global to local coor-
202 dinates (.get_local_coords()); (2) getting x, y, and z coordinates for cell centers (.xcellcenters,
203 .ycellcenters, .zcellcenters, and .xyzcellcenters) and vertices (.xvertices, .yvertices, .zvertices,
204 and .xyzvertices); (3) intersecting a list of xy pairs with the grid and returning the appropriate
205 cellid (.intersect()). Other interesting grid object properties and methods include generating a
206 grid object from a MODFLOW 6 binary grid file (.from_binary_grid_file()), calculating the cell
207 thickness for each cell (.thick), and the saturated thickness for each cell .saturated_thick.
208 The ability to develop model grid types using FloPy allows for innovation in the way a study area
209 is discretized in order to tailor the grid to the needs of the study. For example, Guira \(2018\) used a
210 Voronoi grid to add additional resolution in the vicinity of irrigation wells in the Frenchman Creek Basin
211 in Nebraska, USA to quantify the effects of land-use change and irrigation on streamflow depletion.
212 Furthermore, the ability to develop multi-model simulations using FloPy allows higher-resolution inset
213 models to be added in focused areas. Fienen et al. \(2022\) used focused inset models implicitly coupled
214 to a coarse regional model and solved as a single system of equations to better represent lakes and
215 quantify lake/groundwater interactions in the Central Sands region in Wisconsin, USA. Inset models
216 of lakes in Fienen et al. \(2022\) were developed using modflow-setup (Leaf and Fienen 2022), which
217 relies on FloPy functionality to generate MODFLOW 6 datasets.
```

### 218 3.3 Geospatial Processing

219 Geospatial processing is often a fundamental part of creating a groundwater model. New geospatial
 220 processing functionality has been added to FloPy to help users construct models using data from
 221 common input sources. The geospatial processing functionality has been implemented to work with
 222 the different types of model grids so that it is straightforward to build and construct models with
 223 different grid resolutions or grid types. The geospatial processing routines work with all three of the
 224 model grid types (StructuredGrid, VertexGrid, and UnstructuredGrid).

225 A common geospatial processing task is resampling of raster data onto a model grid. For example,
 226 it is often necessary as part of model construction to resample a raster data set of land surface elevation
 227 onto a model grid. FloPy includes a new raster sampling utility based on the Rasterio Python package
 228 ([Gillies et al. 2013](#)). The following Python code demonstrates the steps for resampling an Esri ASCII
 229 raster format grid onto a Voronoi grid.

```
230 >>> fine_topo = flopy.utils.Raster.load("./grid_data/fine_topo.asc")
```

```
231 >>> top_vg = fine_topo.resample_to_grid(voronoi_grid, band=fine_topo.bands[0],  
232 ... method="linear", extrapolate_edges=True)  
233 ...
```

234 The result of raster resampling is a numpy array, equal in size to the number of cells in the Voronoi  
235 grid, with an interpolated land surface elevation for each model cell. In this Python code example, the  
236 land surface grid was interpolated to the Voronoi grid using a “linear” method, however, the method  
237 also supports other options (nearest, cubic, mean, median, min, and max) for resampling. The color  
238 floods of elevation in Figure 2 show the results of linear raster resampling for land surface onto a variety  
239 of structured and unstructured model grids.

240 Performing intersections of hydrologic features with the model grid is another common modeling  
241 task. FloPy is now equipped with robust and efficient capabilities for intersecting a model grid with  
242 points, lines, and polygons. The underlying intersection routines rely on the Shapely Python package  
243 (Gillies 2022) to determine intersection properties. When a point or collection of points is intersected  
244 with a model grid, the grid intersection routine returns the cells that intersect with the points. When  
245 a line or collection of lines is intersected with a model grid, the grid intersection routine returns the  
246 cells that intersect with the lines and the lengths of lines within the cell. The line and grid intersection  
247 routine also creates and returns individual line segments of the line features within each intersected cell.  
248 When a polygon or collection of polygons is intersected with a model grid, the grid intersection routine  
249 returns the cells that intersect with the polygons and the polygon area within the cell. The polygon and  
250 grid intersection routine also creates and returns individual polygons of the original polygon features  
251 within the intersected cells.

252 The following Python code demonstrates the steps for identifying the grid cells that intersect with  
253 a collection of line segments.

```
254 >>> ixs = flopy.utils.GridIntersect(voronoi_grid, method="vertex")  
255 >>> cellids = []  
256 >>> for points in segments:  
257 ...     segment = ixs.intersect(LineString(points), sort_by_cellid=True)  
258 ...     cellids += segment["cellids"].tolist()
```



260 The result of this code snippet is a list of Voronoi grid cell numbers (called “cellids”) that intersect  
261 with the model grid. The `ixs.intersect()` method also returns the “lengths” of the shapely  
262 collection intersecting each cell, the “vertices” corresponding to each cell that intersects a collection  
263 of shapely objects, and a shapely object (“ixshape”) each portion of the original shapely collection  
264 that intersects a cell. Results of the grid intersection for a linear stream network and the six different  
265 model grids is shown in Figure 3.

## 266 3.4 Processing MODFLOW 6 output

267 MODFLOW 6 has many different types of output that can be created during a simulation. A GWF  
268 Model, for example, can write simulated heads and detailed budget information to binary files. Global  
269 model budgets can be written to comma-separated value text files. Some individual GWF and GWT  
270 Model advanced stress packages can also write simulated output during a simulation. For example,  
271 the Lake (LAK) Package can write simulated lake stages and detailed lake budget information to  
272 binary files. Likewise, the Multi-Aquifer Well (MAW) Package can write simulated well head and well  
273 budgets to binary files. Recent improvements have been made to FloPy to allow users easier access

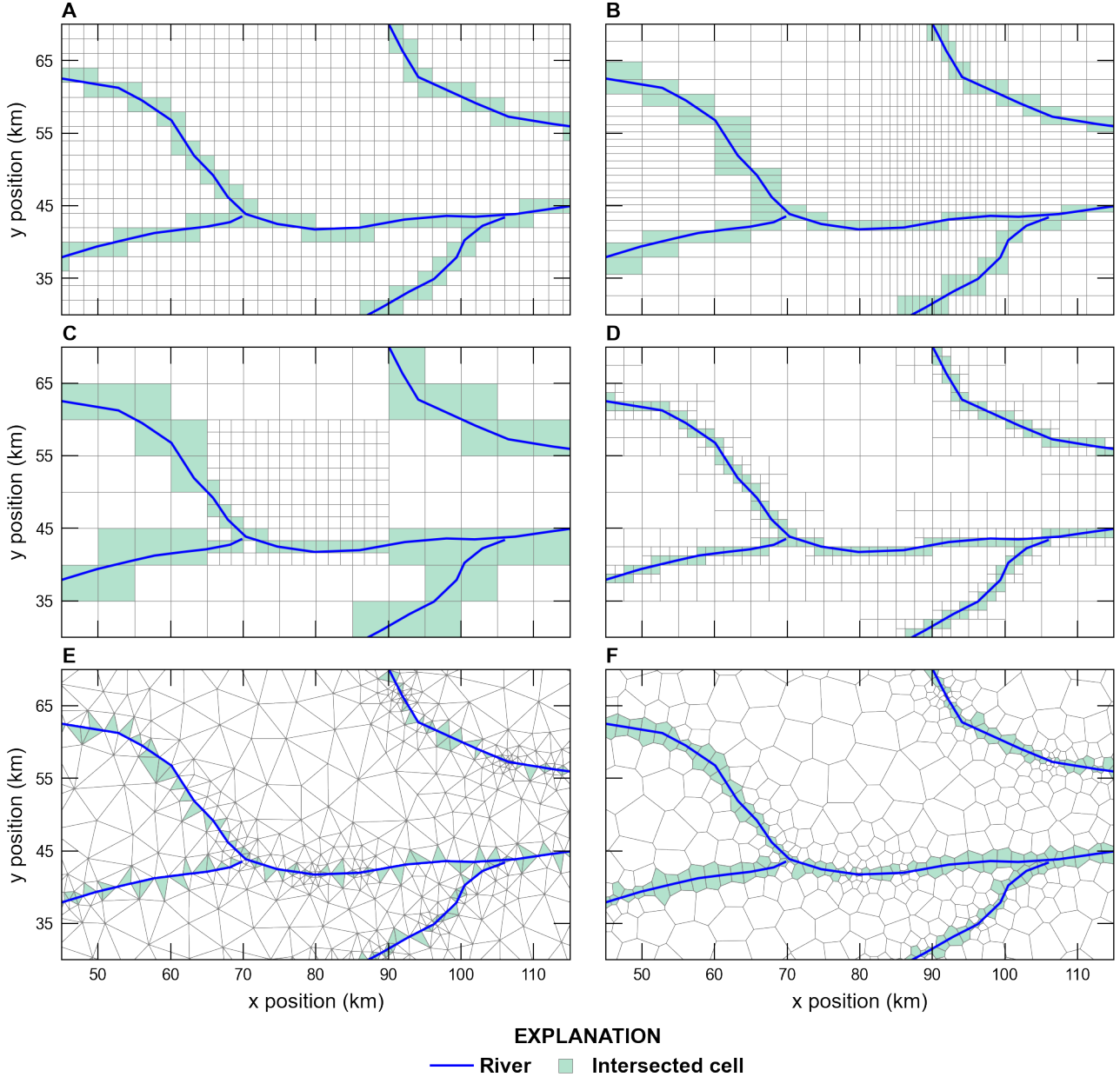


Figure 3: Examples of the intersection of a linear stream network with the model grids shown in Figure 2. Intersections were performed using FloPy for (A) a regular MODFLOW grid, (B) a regular MODFLOW grid with variable row and column spacing, (C) a regular MODFLOW child grid nested within a regular MODFLOW parent grid, (D) a quadtree grid, (E) a triangular grid, and (F) a Voronoi grid. Shaded cells represent those cells that intersect with the linear stream network. Individual plots in this figure are centered on the location of the child grid shown in Figure 2C.

274 to simulation results using `.output` routines. Prior to these improvements, users were required to  
 275 instantiate head, concentration, and budget file readers using file paths and names in order to access  
 276 this information. With the `.output` routines, the readers are automatically generated when called by  
 277 the user.

278       The following `.methods()` syntax shows how a user can discover the type of output information  
279       that is available for the specified `gwf` model.

```
280     >>> gwf.output.methods()  
281     ['list()', 'zonebudget()', 'budget()', 'budgetcsv()', 'head()']
```

282       The `.list()` method can be used to get the incremental (`incremental=True`) or cumulative budget  
283       information for the `gwf` model for a user-specified simulation time, zero-based time step–stress period  
284       tuple, or zero-based index. The `.zonebudget` method allows the user to easily build a Zone Budget for  
285       MODFLOW 6 instance, then run the Zone Budget program, and view output. The `.budget()` method  
286       gives user access to data in binary MODFLOW 6 cell-by-cell budget files. The `.budgetcsv()` method  
287       gives user access to cumulative and incremental global budget data saved to a comma separated values  
288       file. The `.head()` method gives user access to data in the binary MODFLOW 6 head file.

289       Similarly, The following `.methods()` syntax shows how a user can discover the type of output  
290       information that is available for advanced stress packages like the LAK package.

```
291     >>> gwf.lak.output.methods()  
292     ['zonebudget()', 'budget()', 'budgetcsv()', 'package_convergence()', 'obs()',  
293     'stage()']
```

294       The `.package_convergence()` method can be used to get the convergence information for an advanced  
295       stress package. The `.obs()` method can be used to get observation data saved for a model or stress  
296       package as a numpy record array or pandas data frame. The `.stage()` method is the dependent  
297       variable for the LAK package and is equivalent to the `.head()` method for the `gwf` model.

### 298       **3.4.1 Processing simulated dependent-variable data**

299       Dependent-variable data (for example, head or concentration) for a MODFLOW 6 groundwater flow  
300       or transport model can be accessed using the `.output()` method on the GWF or GWT model, re-  
301       spectively. To access the simulated head output, for example, a call can be made to the head reader  
302       to retrieve data for a specified simulation time using the `.get_data()` method as follows.

```
303     >>> head = gwf.output.head().get_data(totim=1.0)
```

304       In this case, the `head` variable is a numpy array equal in size to the size of the model grid. Head data  
305       can also be accessed for a zero-based time step–stress period tuple

```
306     >>> head = gwf.output.head().get_data(kstpkper=(0,0))
```

307       or a zero-based index

```
308     >>> head = gwf.output.head().get_data(idx=0)
```

309       in addition providing a user-specified simulation time (`totim=`).

310 **3.4.2 Processing simulated cell-by-cell budget results**

311 Similar to head output, cell-by-cell budget information can be accessed using FloPy. Unlike the  
312 simulated head file, the cell-by-cell budget file can have data for more than one item, which can be  
313 either arrays or lists of data. The data in the cell-by-cell budget file can be determined using

```
314 >>> gwf.output.budget().list_unique_records()
315 RECORD           IMETH
316 -----
317 FLOW-JA-FACE     1
318 DATA-SPDIS      6
319 DATA-SAT        6
320 WEL             6
321 DRN             6
322 RCHA            6
323 EVTA            6
324 SFR             6
325 LAK             6
```

326 The IMETH code indicates if the data is an array (IMETH=1) or is list based (IMETH=6). Cell-by-cell  
327 specific-discharge data can be extracted using

```
328 >>> spdis = gwf.output.budget().get_data(totim=1.0, text="DATA-SPDIS")[0]
```

329 Specific-discharge data is returned as a list containing a Numpy record array for the user-specified  
330 simulation time (totim=). Like MODFLOW head data, all of the data in the cell-by-cell data file for  
331 a user-specified simulation time (totim=), zero-based time step-stress period tuple (kstpkper=), or  
332 zero-based index (idx=) can also be extracted. Specific-discharge data can be processed into a form  
333 that can be plotted with FloPy using

```
334 >>> qx, qy, qz = flopy.utils.postprocessing.get_specific_discharge(spdis, gwf,
335 ... head=head)
```

336 The optional argument head= above sets the specific-discharge in inactive or dry cells to NaN. The  
337 get\_specific\_discharge() method also includes functionality to plot specific discharge values at the  
338 cell "centers" (default), "faces", or "vertices".

339 **3.4.3 Performing zone budgets analyses**

340 zonebudget() output methods are available for both the gwf model and the gwf.lak advanced stress  
341 package examples shown above since they both solve a continuity equation. The other flow and  
342 transport advanced stress packages also solve continuity equations and can be used with this Zone  
343 Budget functionality. The zonebudget() output method can be used to perform a Zone Budget  
344 analysis on the LAK advanced stress package using

```
345 >>> zonbud = gwf.lak.output.zonebudget(zarr)
```

```

346     >>> zonbud.write_input()
347     >>> zonbud.run_model()
348     FloPy is using the following executable to run the model: zbud6
349             ZONEBUDGET Version 6
350             U.S. GEOLOGICAL SURVEY
351             VERSION 6.3.0 03/04/2022
352             .....
353             Normal Termination
354             (True, [])

```

355 `zarr` in the `gwf.lak.output.zonebudget()` is a numpy array that defines an integer zone for each  
 356 lake in the LAK advanced stress package. Zone Budget output can be returned as a numpy record  
 357 array (`.get_budget()` or `get_volumetric_budget()`) or a `panda` dataframe (`get_dataframes()`).

### 358 3.5 Plotting

359 FloPy plotting functions presented in Bakker et al. (2016) have been updated to support plotting  
 360 both structured and unstructured models in map and cross-section view using the `.PlotMapView()`  
 361 and `.PlotCrossSection()` classes, respectively. The plotting methods are thin wrappers around the  
 362 matplotlib plotting methods (Hunter 2007) and allow fine-grained control using matplotlib keyword  
 363 arguments (`kwargs`). The following Python code demonstrates the steps for plotting a map of simulated  
 364 heads, the model grid, the location of drain (DRN) package cells, specific-discharge vectors, and head  
 365 contours for the `gwf` model.

```

366     >>> mm = flopy.plot.PlotMapView(model=gwf)
367     >>> mm.plot_array(head, edgecolor="0.5")
368     >>> mm.plot_bc("DRN")
369     >>> mm.plot_grid()
370     >>> cs = mm.contour_array(head)
371     >>> mm.ax.clabel(cs)
372     >>> mm.plot_vector(qx, qy, normalize=True)
373     >>> plt.show()

```

374 Figure 4A shows the outcome of the Python code demonstrated above with additional geographic  
 375 features and fine-grained control of grid lines, text, annotations, tick locations, and axis labels. Results  
 376 shown in Figure 4 are for a steady-state model discretized into three convertible layers, with isotropic  
 377 hydraulic properties, a hydraulic conductivity of 1 m/d, with rivers represented a drain cells, with  
 378 drains located on the top of the model in layer 1 to prevent groundwater levels from exceeding the  
 379 top of the model, and with an areal recharge rate of 0.000001 m/d. Figure 4B shows use of the  
 380 `.plot_array()` method to create a map of the layer containing the water table, drain cells where the  
 381 groundwater is discharging to a river, and cells where groundwater is discharging to the surface.

382 The following Python code demonstrates the steps for plotting a cross-section of simulated heads  
 383 and the model grid for the `gwf` model along an arbitrary line defined using a list of x, y coordinate  
 384 pairs (tuples) defining the vertices of the line. For structured grids, cross-sections can also be specified  
 385 along a row or column.

```

386     >>> fx = flopy.plot.PlotCrossSection(model=gwf,

```

```

387 ... line={"line": [(0, 42500), (186801, 42500)]})
388 ...
389 >>> fx.plot_array(head, head=head)
390 >>> fx.plot_grid()
391 >>> plt.show()

```

The `head=` keyword option `plot_array()` method in the Python code demonstrated above limits the color flood to the saturated thickness of water in each cell. Figure 4C and D show the outcome of the Python code demonstrated along cross-section lines A–A' and B–B' (shown in Figure 4A) above with fine-grained control of grid lines, text, annotations, tick locations, and axis labels. Note that the color flood of head in Figure 4C and D shows that unconfined conditions occur in higher elevation cells or cells adjacent to river cells.

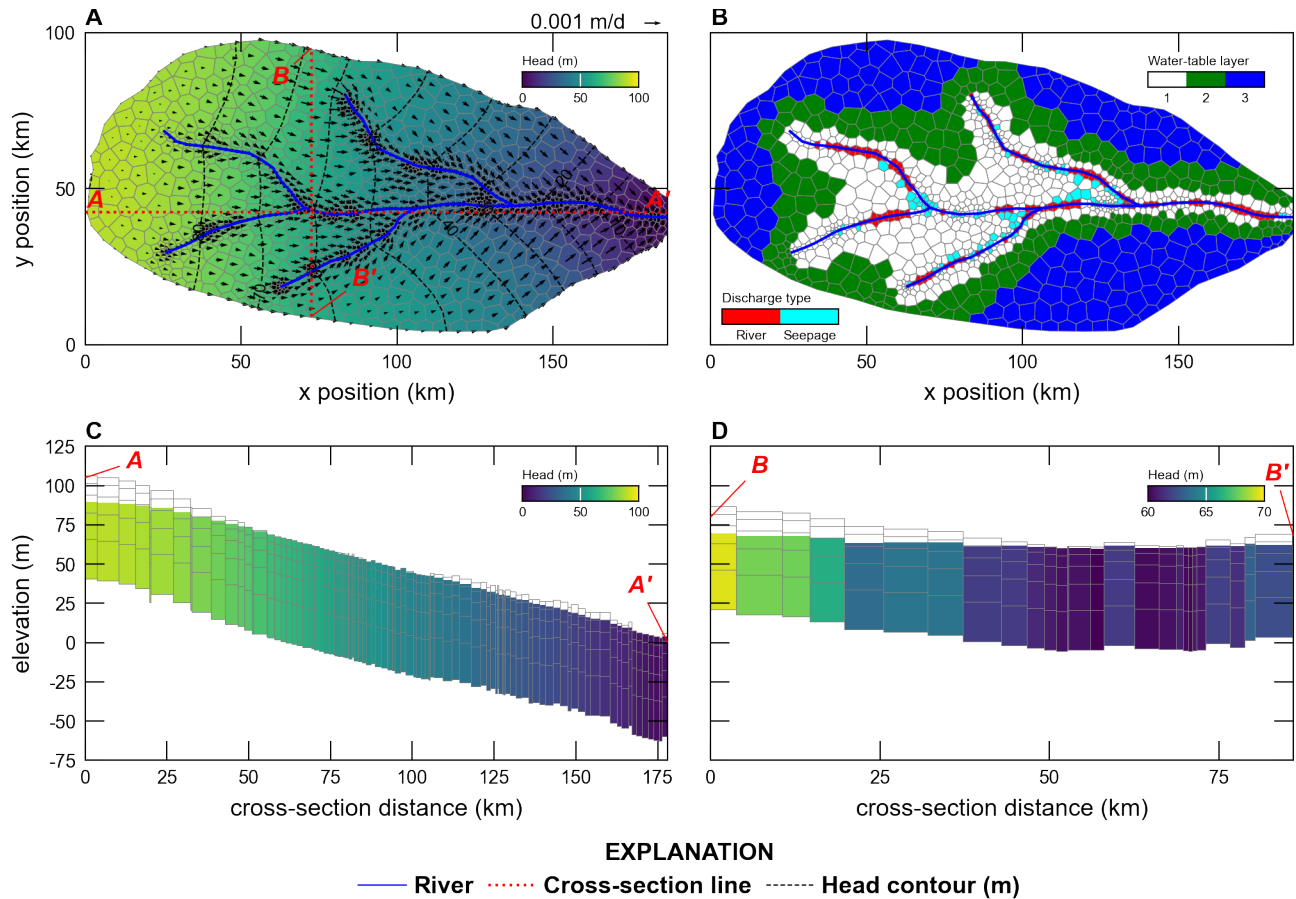


Figure 4: Examples of FloPy map and cross-section plotting capabilities for a model discretized using a Voronoi grid (Figure 2F). (A) Map showing simulated heads and specific-discharge vectors in the upper-most saturated cells. (B) Map showing the layer containing the water table, the location of cells where the aquifer is **discharge** to rivers represented as drain cells, and the location of cells where groundwater is discharging to the land surface. (C) East-West cross-section along line A–A', shown on Figure 4A, showing the model grid, simulated heads, and cells where water-table conditions exist. (D) North-South cross-section along line B–B', shown on Figure 4A, showing the model grid, simulated heads, and cells where water-table conditions exist.

### 398 3.6 Exporting Grid Data to Other Formats

399 Model input and output can be exported in a variety of standard formats using the `export()` method,  
400 which is available for FloPy model objects, package objects, binary dependent-variable (head, con-  
401 centration, *etc.*), and cell-by-cell output files. Standard output formats that are currently supported  
402 include shapefiles ([ESRI 1998](#)), NetCDF files ([Rew et al. 2006](#); [Rew and Davis 1990](#)), and Visualiza-  
403 tion Tool Kit (VTK) files ([Schroeder et al. 2006](#)). Entire models, packages, individual package arrays,  
404 binary dependent-variables (for example heads), or three-dimensional representations of binary cell-by-  
405 cell data can be exported. Shapefile and VTK output can be exported for all grid types but NetCDF  
406 files can currently only be exported for structured grids. The NetCDF output capability has been used  
407 to convert entire models and associated output so that it can be rendered in the GWWebFlow viewer  
408 ([U.S. Geological Survey 2018](#)).

409 The following Python code demonstrates the steps for exporting the `gwf` model as a VTK dataset  
410 with flat cell tops and bottoms (stair-case representation).

```
411 >>> gwf.export("temp_vtk/vtk_smooth", fmt='vtk', smooth=False,  
412 ... vertical_exaggeration=500.0, pvd=True)  
413 ...
```

414 VTK models can also be exported with smooth cell tops and bottoms using elevations interpolated to  
415 the cell vertices. Other supported export formats can be created by specifying the file extension to be  
416 `.shp` for shapefiles, `.nc` for NetCDF files, or if the `fmt` keyword is `vtk` (as shown above) for VTK files.  
417 Figure 5 shows stair-case and smooth VTK exports of the model described in Section 3.5 and rendered  
418 with Paraview ([Ahrens et al. 2005](#)).

## 419 4 Scripting MODFLOW 6 Model Development Using Python and 420 FloPy

421 In this section, FloPy is used to construct, run, and post process a MODFLOW 6 model. All pre-  
422 and post-processing was done using FloPy grid, geospatial processing, MODFLOW 6 processing, and  
423 plotting functionality discussed previously.

424 Hill et al. (1998) presented a synthetic test case (Synthetic Valley) of an undeveloped alluvial valley  
425 surrounded by low permeability bedrock. The model included the Blue Lake and Straight River surface  
426 water features (Figure 6A). The model presented in Hill et al. (1998) was simulated using MODFLOWP  
427 ([Hill 1992](#)) using a structured grid with a constant 152.4 m grid spacing, three model layers, and 1,000  
428 active cells per layer. The upper two layers represented an unconfined aquifer, and the third layer  
429 represented a lower aquifer unit that is separated from the overlying aquifer by a confining unit in the  
430 northern part of the model domain (Figure 6A). The confining unit was not explicitly represented in  
431 Hill et al. (1998), instead a quasi-3D approach (low vertical conductance) between layers 2 and 3 was  
432 used to represent the confining unit.

### 433 4.1 MODFLOW 6 Model Setup

434 To demonstrate that capabilities of FloPy and MODFLOW 6 the 6,096 m x 3,810 m model domain  
435 is discretized using a Voronoi grid, with 6,343 active cells per layer, and the discretization by ver-  
436 tices (DISV) package (Figure 6A). The model grid was developed using the FloPy `Triangle()` and  
437 `VoronoiGrid()` utility classes. The model grid was refined within Blue Lake, around Straight River  
438 using a 750 m buffer length, and around pumping wells P1, P2, and P3 using a 100 m buffer length.

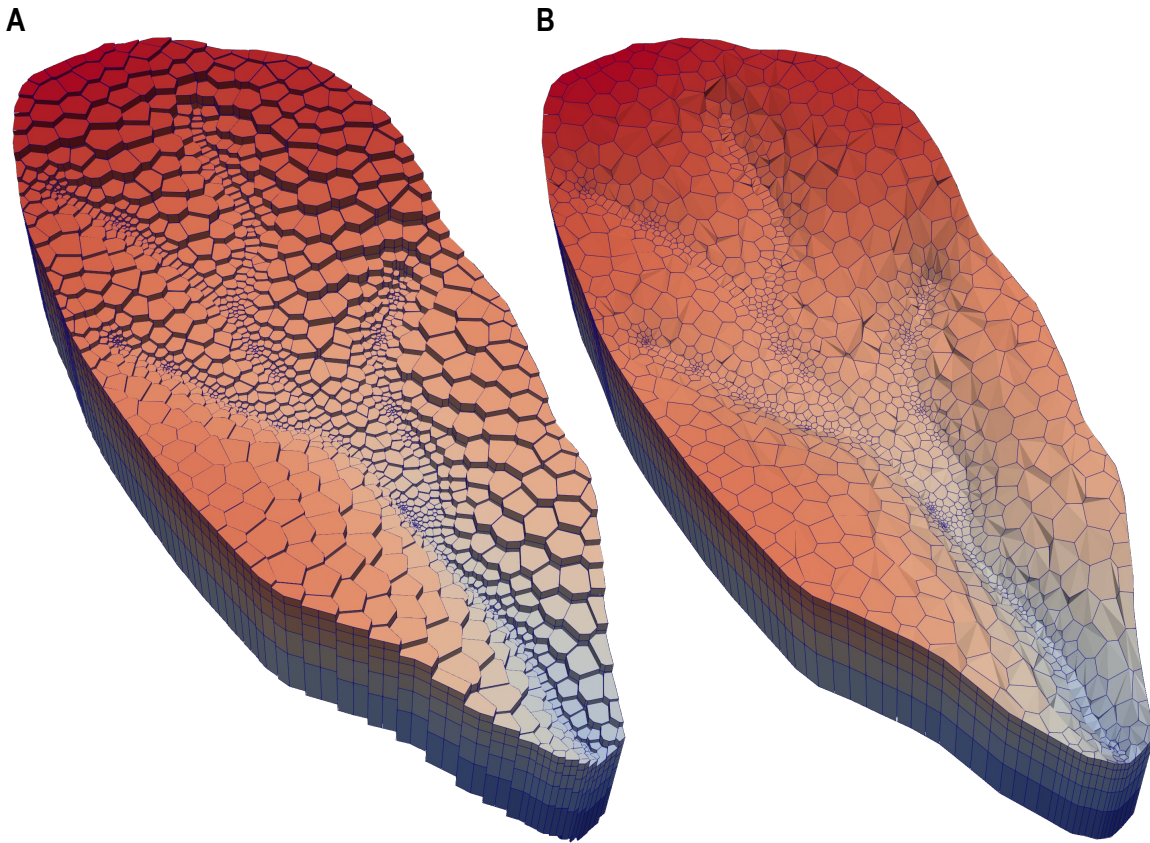


Figure 5: Two different graphical renderings of the Voronoi model grid: (A) stair-cased representation in which cell have flat tops and bottoms and (B) smooth representation in which elevations for cell vertices are interpolated using cell top and bottom elevations. Renderings were created using Paraview (Ahrens et al. 2005) and Visualization Tool Kit (Schroeder et al. 2006) files exported from FloPy.

In this example both groundwater flow and solute transport are simulated. As a result, the lower aquifer has been discretized into 3 layers (instead of one) to better represent solute transport. Confining units have to be explicitly simulated in MODFLOW 6, therefore, a total of six layers are simulated. The bottom of layers 1, 2, 3, and 4 were set to constant values of -1.53, -15.24, -15.55 and -30.48 m, respectively. In areas where the confining unit does not exist, the IDOMAIN concept (Langevin et al. 2017) was used to eliminate cells in model layer 3 (by setting IDOMAIN=-1) where the confining unit does not exist. In these areas, the bottom of layer 2 was set equal to the bottom of layer 3 (-15.55 m) and idomain was set to -1. The assignment of IDOMAIN equal to -1 marks these cells in layer 3 as “vertical pass through cells,” which means an overlying cell in layer 2 is directly connected to an underlying cell in layer 4.

The bottom of the model (layer 6) is based on Hill et al. (1998) and the bottom of layer 5 was specified to be half the distance between the bottom of layers 4 and 6. The top of the model was developed from topographic contours developed for model that was used as the starting point for Hill et al. (1998) (Pollock 2014); the top of the model is shown in Figure 7A. The top of the model and the bottom of layers 6 were resampled from the data used in the structured grid model using the `.resample_to_grid()` method and linear interpolation. Figure 9 shows the vertical discretization along cross-section lines A-A' and B-B', which are shown in Figure 7A. The groundwater flow and

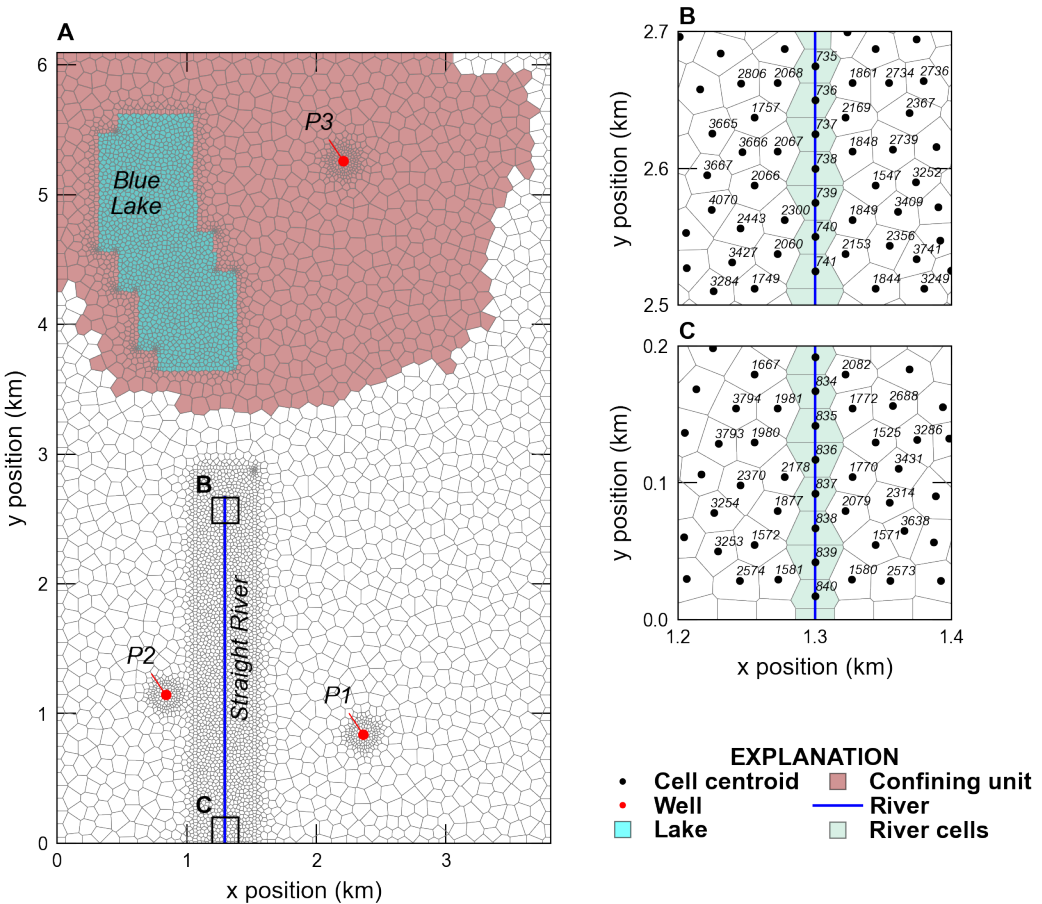


Figure 6: Synthetic Valley model used to demonstrate the MODFLOW 6 capabilities of FloPy. (A) Map showing the Voronoi grid used to discretized the model domain and the location of Blue Lake, Straight River, and the areal extent of the confining unit separating the upper and lower aquifer units. (B) Map showing model cells intersecting the northern end of Straight River. (C) Map showing model cells intersecting the southern end of Straight River. The cell centroid and cell numbers in the inset areas at the northern and southern end of Straight River are also shown on (B) and (C).

456 transport models were run for a total of 30 years. The groundwater flow model used a single steady-  
 457 state time step and groundwater flow results were used to run the transport model with a total of 360  
 458 time steps with a constant length of 30.4375 days.

459 Hydraulic properties for the model were resampled from the data used in the structured grid model  
 460 that was used as the starting point for Hill et al. (1998) (Pollock 2014). The horizontal hydraulic con-  
 461 ductivity was discretized into five zones with values of 45.72, 50.29, 60.96, 83.82, and 121.92 m/d; the  
 462 lowest hydraulic conductivity zone was located south of Blue Lake and the highest hydraulic conduc-  
 463 tivity zone was located beneath Blue Lake. The vertical hydraulic conductivity in the upper and lower  
 464 aquifer was specified to be one quarter of the horizontal hydraulic conductivity. The horizontal and

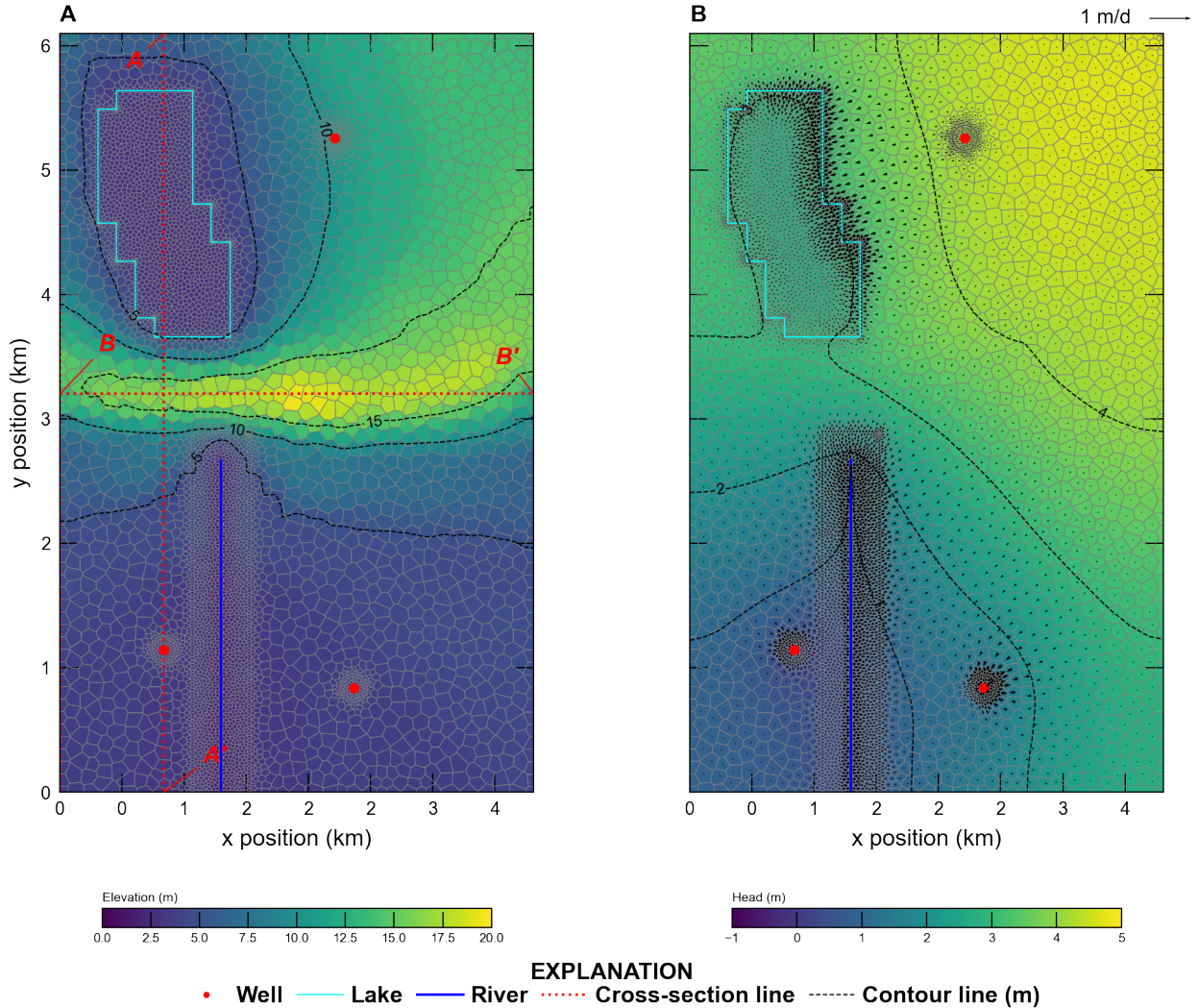


Figure 7: Map showing Synthetic Valley model (A) topography and (B) simulated steady-state heads and specific discharge rates in model layer 1. Cross-section lines A–A' and B–B' shown in Figure 9 are also shown on (A).

vertical hydraulic conductivity in the confining unit was set equal to  $9.14 \times 10^{-4}$  m/d. The horizontal and vertical hydraulic conductivity were resampled from the data used in the structured grid model using the `.resample_to_grid()` method and the nearest neighbor algorithm.

For the groundwater transport model the porosity was set to 0.2 in the upper and lower aquifer and 0.4 for cells in the confining unit. For the transport model, the Total Variation Diminishing scheme was used to simulate advection. Dispersion was simulated using a longitudinal dispersivity of 75 m and a transverse dispersivity of 7.5 m. Molecular diffusion was not represented.

In the Hill et al. (1998) representation of Synthetic Valley, the Straight River was simulated as head-dependent river (RIV) package cells, and Blue Lake was simulated as a high-hydraulic conductivity feature in model layer 1. In this FloPy recreation, Straight River is simulated using the streamflow routing (SFR) package, and Blue Lake is simulated using the LAK package. The location of the cells in model layer 1 with SFR or LAK package cells were determined using `GridIntersect().intersect()`

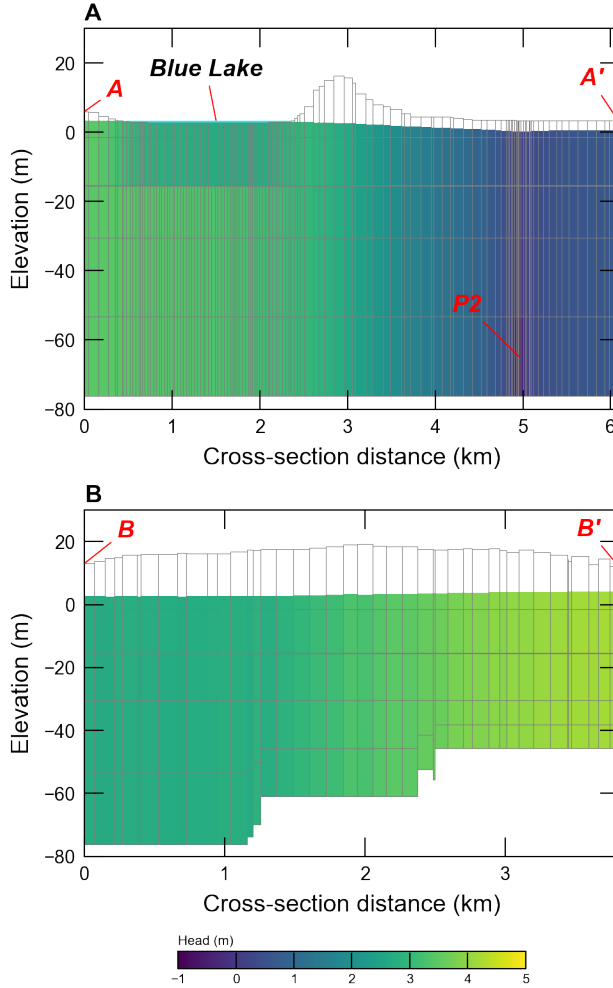


Figure 8: Cross-section of Synthetic Valley model grid and simulated steady-state heads along cross-section line (A) A–A' and (B) B–B'. The simulated Blue Lake steady-state stage (3.46 m) and pumping well P-2 are also shown on (A).

477 FloPy functionality (Figure 7A).

478 Straight River was discretized into 108 SFR reaches. Cells that intersect the northern and southern  
 479 end of Straight River are shown in Figures 7B and C. The bed thickness and width of each SFR reach  
 480 was specified to be 0.3048 and 3.048 m, respectively. The leakance for each SFR reach was calculated  
 481 using the bed thickness, reach width, and reach length in each cell and based on a total Straight River  
 482 conductance of  $50,971.72 \text{ m}^2/\text{d}$ . A specified rainfall rate of  $0.0025 \text{ m/d}$  and a potential evaporation  
 483 rate of  $0.0019 \text{ m/d}$  was defined for each Straight River reach.

484 Blue Lake was simulated as a lake on top of the model grid and only had vertical connections to  
 485 1,406 cells in the underlying upper aquifer (model layer 1). A bed leakance of  $0.0013 \text{ l/d}$  was specified  
 486 for each cell connected to Blue Lake. A specified rainfall rate of  $0.0025 \text{ m/d}$  and a potential evaporation  
 487 rate of  $0.0019 \text{ m/d}$  was defined for Blue Lake.

488 Drain (DRN) cells were specified in each cell in model layer 1 that was not connected to Blue Lake  
 489 to prevent water levels from exceeding the top of the model. The conductance of each DRN cell was  
 490 based on the horizontal cell area, a thickness of 0.3048 m, and a vertical hydraulic conductivity of  
 491  $0.03048 \text{ m/d}$ . The drainage conductance was scaled from 0 to 100% of the specified conductance from

492 1 m below the top of the model to the top of the model, respectively.

493 Areal specified recharge and potential evapotranspiration rates of 0.0025 and 0.0019 m/d were  
494 specified using the recharge (RCH) and evapotranspiration (EVT) packages, respectively. The EVT  
495 surface was specified to be the top of the model and the EVT extinction depth was specified to be 1  
496 m.

497 The location of pumping wells P1, P2, and P3 were determined using `GridIntersect().intersect()`  
498 FloPy functionality (Figure 7A). Pumping rates of -7,600, -7,600, and -1,900 m<sup>3</sup>/d were specified for  
499 pumping wells P1, P2, and P3, respectively.

500 Transport was not simulated in the LAK and SFR packages. Instead, a specified concentration  
501 condition with a concentration of 1.0 mg/L was specified for Blue Lake. All other stress packages were  
502 assumed to have a concentration of 0 mg/L.

503 An initial head of 11 m was specified for every cell. An initial stage of 3.44 m was specified for  
504 Blue Lake. An initial concentration of 0 mg/L was specified for the transport model.

## 505 4.2 Simulated Results

506 Simulated heads and vectors of specific discharge in model layer 1 are shown in Figure 7B. Specific  
507 discharge is greatest on the east side of Blue Lake and in the vicinity of the three pumping wells and  
508 Straight River. Cross-sections showing simulated heads along cross-sections A–A' and B–B' are shown  
509 in Figure 9. The cross-sections show that water table conditions occur in most of the model domain  
510 except in the vicinity of Blue Lake.

511 Simulated concentrations at the end of 30-years in all six model layers are shown in Figure 9.  
512 Simulated concentrations are highest beneath Blue Lake in model layer 1 and do not vary much in  
513 model layers 1 and 2. Simulated concentrations in model layer 3 are limited to the extent of the  
514 confining unit because the remaining cells in the layer are defined to be vertical pass through cells  
515 (`IDOMAIN=-1`). The lateral extent of the solute plume does not vary much south of Blue Lake because  
516 of the lack of confinement in these areas.

## 517 5 Summary and Conclusions

518 FloPy is a popular Python package for building, running, and post processing groundwater models. It  
519 is open source and developed with input from a growing community of contributors. This paper sum-  
520marizes important new FloPy capabilities that have been added since the package was first described  
521 by (Bakker et al. 2016). The new capabilities can be summarized as follows.

522 • FloPy supports the creation of many different types of groundwater models, including mod-  
523 els that use MODFLOW 6, MODFLOW-2005, MODFLOW-NWT, MODFLOW-USG, MT3D,  
524 MT3D-USGS, and SEAWAT. FloPy support for MODFLOW 6 is based on an entirely new ap-  
525 proach designed to automatically support all MODFLOW 6 models, packages, and options. The  
526 underlying FloPy classes for MODFLOW 6 are programmatically generated from the same input  
527 definition files that are used to construct the MODFLOW 6 user guide. This correspondence  
528 ensures that the FloPy classes are in direct correspondence with MODFLOW 6 input.

529 • FloPy has been extended to support unstructured model grids in addition to regular grids defined  
530 by layers, rows, and columns. FloPy has several different routines for creating unstructured grids.  
531 FloPy includes a wrapper for the GRIDGEN program (Lien et al. 2014), which can be used to  
532 create layered quadtree grids. FloPy also includes a wrapper for the Triangle program (Shewchuk  
533 1996), which can be used to create triangular meshes. A triangular mesh can be converted by  
534 FloPy into a Voronoi grid. Grid information is stored for each FloPy model created by the user.

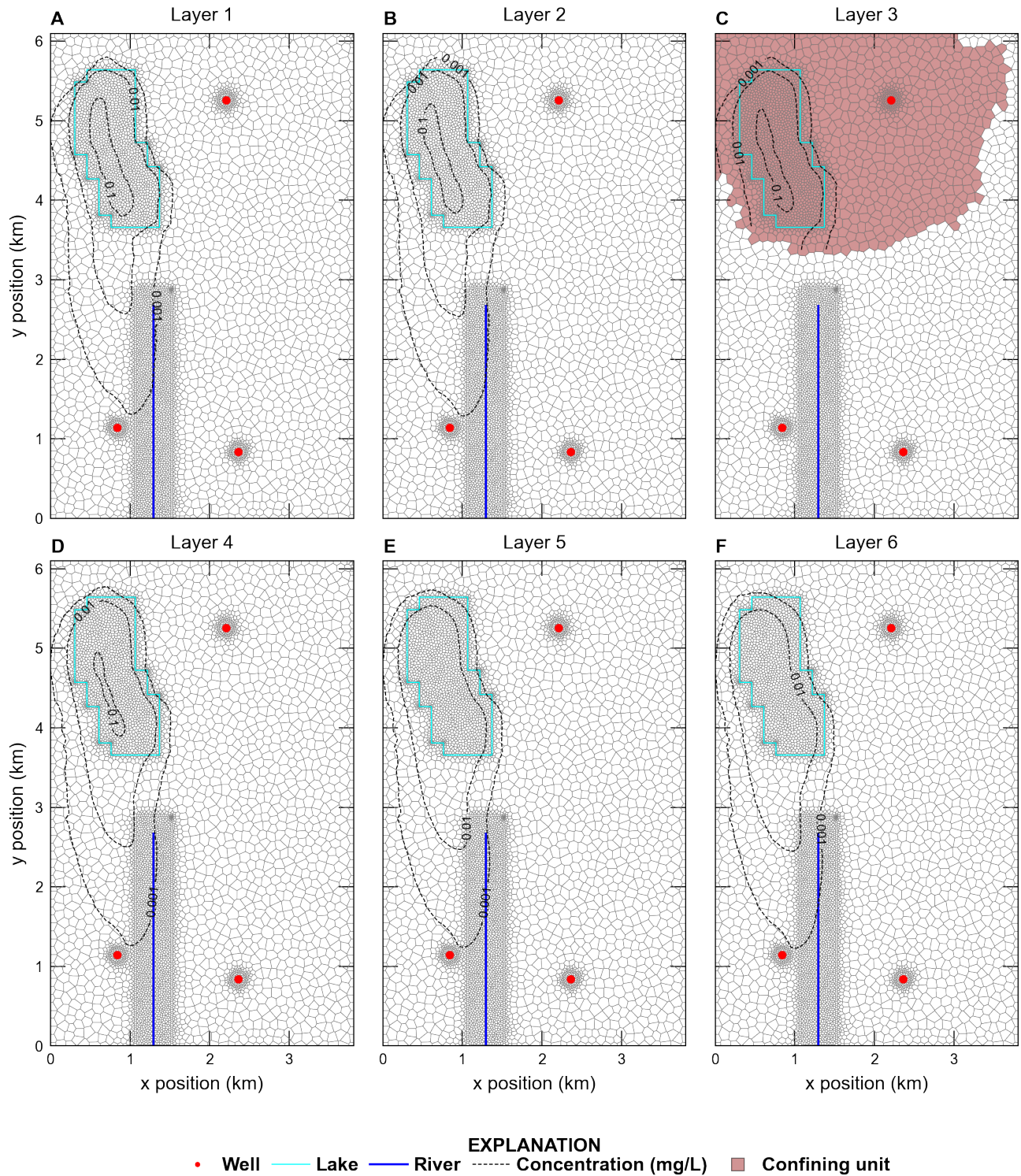


Figure 9: Maps showing Synthetic Valley simulated concentrations at the end of 30 years in model layer (A) 1, (B) 2, (C) 3, (D) 4, (E) 5, and (F) 6. The extent of the confining unit in model layer 3 is also shown on (C).

535 This model grid object is used systemically throughout FloPy for geospatial operations, plotting,  
536 and exporting model information to supported formats.

- 537 • Geospatial intersections of points, lines, and polygons with model grids and raster resampling  
538 onto model grids are common steps in model construction. FloPy fully supports these geospatial  
539 operations through its grid intersection and raster resampling routines.
- 540 • Access to model output using FloPy has been simplified for MODFLOW 6 models. The new  
541 output access routines makes it possible to quickly extract simulated results from binary and  
542 text model output files.
- 543 • FloPy supports plan-view map and cross-section plotting of model grids, boundary conditions,  
544 and simulated results. These plotting routines work with structured and unstructured models  
545 and can be customized to produce high quality figures.
- 546 • FloPy supports the export of model information to shapefiles, VTK files, and NetCDF files. These  
547 exported files can then be loaded into other software programs, such as geographic information  
548 systems or advanced visualization programs for additional processing.

549 FloPy makes it possible to construct, and reproduce the construction, of a groundwater model  
550 from native data in any format that can be accessed using Python. The robust new features in FloPy  
551 allow users to quickly try different model grids, different model spatial and temporal resolution, and  
552 different model configurations.

553 It is often useful to write a Python script to construct a groundwater model from start to finish.  
554 The new geospatial processing routines make it possible to change model resolution as part of the  
555 model construction script. This allows one to prototype fast running models with coarse resolution  
556 and use finer resolution as the model starts to behave as intended. This workflow also allows one to  
557 conduct grid convergence studies to ensure that the grid is not the cause of unintended model behavior.

## 558 Acknowledgments

559 The authors gratefully acknowledge the efforts of Mark Bakker and Vincent E.A. Post for initially  
560 developing FloPy and their continued efforts improving FloPy. Funding for this research was provided  
561 by the Enterprise Capacity (EC) project of the U.S. Geological Survey Integrated Water Prediction  
562 program.

## 563 Data Availability Statement

564 FloPy is an open source software product and we welcome bug reports, code contributions, or im-  
565 provements to the documentation from the community. The FloPy Python package can be installed  
566 using `conda` or `pip`. The source code, code documentation, tutorials, and examples can be found in  
567 the [FloPy GitHub repository](#). [The Synthetic Valley example is available as a MODFLOW 6 example](#)  
568 [and the hypothetical watershed grid examples are available on the FloPy GitHub repository.](#)

## 569 References

570 Ahrens, J., B. Geveci, and C. Law. 2005. ParaView: An End-User Tool for Large Data Visualization.  
571 Visualization Handbook. Elsevier.

- 572 Bakker, M., V. Post, C.D. Langevin, J.D. Hughes, J. White, J. Starn, and M.N. Fienen. 2016. Scripting  
573 MODFLOW model development using Python and FloPy. *Groundwater* 54, no. 5: 733–739, <https://doi.org/10.1111/gwat.12413>.
- 575 Befus, K.M., P.L. Barnard, D.J. Hoover, J.A. Finzi Hart, and C.I. Voss. 2020. Increasing threat of  
576 coastal groundwater hazards from sea-level rise in California. *Nature Climate Change* 10, no. 10:  
577 946–952, <https://doi.org/10.1038/s41558-020-0874-1>.
- 578 Befus, K.M., K.D. Kroeger, C.G. Smith, and P.W. Swarzenski. 2017. The Magnitude and Origin of  
579 Groundwater Discharge to Eastern U.S. and Gulf of Mexico Coastal Waters. *Geophysical Research  
580 Letters* 44, no. 20: 10,396–10,406, <https://doi.org/10.1002/2017GL075238>.
- 581 Burek, P., Y. Satoh, T. Kahil, T. Tang, P. Greve, M. Smilovic, L. Guillaumot, F. Zhao, and Y. Wada.  
582 2020. Development of the Community Water Model (CWatM v1.04) – a high-resolution hydrological  
583 model for global and regional assessment of integrated water resources management. *Geoscientific  
584 Model Development* 13, no. 7: 3267–3298, <https://doi.org/10.5194/gmd-13-3267-2020>.
- 585 Ebeling, P., F. Handel, and M. Walther. 2019. Potential of mixed hydraulic barriers to remediate  
586 seawater intrusion. *Science of The Total Environment* 693: 133478, <https://doi.org/10.1016/j.scitotenv.2019.07.284>.
- 588 ESRI. 1998. ESRI Shapefile Technical Description, an ESRI white paper. <http://www.esri.com/library/whitepapers/pdfs/shapefile.pdf> (accessed August 29, 2022).
- 590 Essawy, B.T., J.L. Goodall, W. Zell, D. Voce, M.M. Morsy, J. Sadler, Z. Yuan, and T. Malik. 2018.  
591 Integrating scientific cyberinfrastructures to improve reproducibility in computational hydrology:  
592 Example for HydroShare and GeoTrust. *Environmental Modelling & Software* 105: 217–229, <https://doi.org/10.1016/j.envsoft.2018.03.025>.
- 594 Fienen, M.N. and M. Bakker. 2016. HESS Opinions: Repeatable research: what hydrologists can learn  
595 from the Duke cancer research scandal. *Hydrology and Earth System Sciences* 20, no. 9: 3739–3743,  
596 <https://doi.org/10.5194/hess-20-3739-2016>.
- 597 Fienen, M.N., M.J. Haserodt, A.T. Leaf, and S.M. Westenbroek. 2022. Simulation of regional ground-  
598 water flow and groundwater/lake interactions in the Central Sands, Wisconsin. Scientific Investigations Report  
599 2022-5046, 111 p. <https://doi.org/10.3133/sir20225046>.
- 600 Gillies, S.. 2022. The shapely user manual. <https://shapely.readthedocs.io/en/stable/manual.html> (accessed August 28, 2022).
- 602 Gillies, S. et al.. 2013. Rasterio: geospatial raster I/O for Python programmers. <https://github.com/rasterio/rasterio> (accessed October 6, 2022).
- 604 Guira, M.. 2018. Numerical Modeling Of The Effects Of Land Use Change And Irrigation On Stream-  
605 flow Depletion Of Frenchman Creek, Nebraska. Master's thesis, University of Nebraska, Lincoln,  
606 NE.
- 607 Hill, M.C.. 1992. A computer program (MODFLOWP) for estimating parameters of a transient, three-  
608 dimensional, ground-water flow model using nonlinear regression. U.S. Geological Survey Open-File  
609 Report 91-484, 358 p.
- 610 Hill, M.C., R.L. Cooley, and D.W. Pollock. 1998. A Controlled Experiment in Ground Water Flow  
611 Model Calibration. *Groundwater* 36, no. 3: 520–535, <https://doi.org/10.1111/j.1745-6584.1998.tb02824.x>.

- 613 Hughes, J.D., C.D. Langevin, and E.R. Banta. 2017. Documentation for the MODFLOW 6 framework.  
614 U.S. Geological Survey Techniques and Methods, book 6, chap. A57, 36 p. <https://doi.org/10.3133/tm6A57>.
- 616 Hughes, J.D., S.A. Leake, D.L. Galloway, and J.W. White. 2022. Documentation for the Skeletal  
617 Storage, Compaction, and Subsidence (CSUB) Package of MODFLOW 6. U.S. Geological Survey  
618 Techniques and Methods, book 6, chap. A62, 57 p. <https://doi.org/10.3133/tm6A62>.
- 619 Hunter, J.D.. 2007. Matplotlib: A 2D graphics environment. *Computing in science & engineering* 9,  
620 no. 03: 90–95.
- 621 Jaxa-Rozen, M., J.H. Kwakkel, and M. Bloemendal. 2019. A coupled simulation architecture for  
622 agent-based/geohydrological modelling with NetLogo and MODFLOW. *Environmental Modelling  
623 & Software* 115: 19–37, <https://doi.org/10.1016/j.envsoft.2019.01.020>.
- 624 Knowling, M.J., J.T. White, and C.R. Moore. 2019. Role of model parameterization in risk-based  
625 decision support: An empirical exploration. *Advances in Water Resources* 128: 59–73, <https://doi.org/10.1016/j.advwatres.2019.04.010>.
- 627 Langevin, C.D., J.D. Hughes, A.M. Provost, E.R. Banta, R.G. Niswonger, and S. Panday. 2017. Doc-  
628 umentation for the MODFLOW 6 Groundwater Flow (GWF) Model. U.S. Geological Survey Tech-  
629 niques and Methods, book 6, chap. A55, 197 p. <https://doi.org/10.3133/tm6A55>.
- 630 Langevin, C.D., S. Panday, and A.M. Provost. 2020. Hydraulic-Head Formulation for Density-  
631 Dependent Flow and Transport. *Groundwater* 58, no. 3: 349–362.
- 632 Langevin, C.D., A.M. Provost, S. Panday, and J.D. Hughes. 2022. Documentation for the MODFLOW  
633 6 Groundwater Transport (GWT) Model. U.S. Geological Survey Techniques and Methods, book 6,  
634 chap. A61, 56 p. <https://doi.org/10.3133/tm6A55>.
- 635 Leaf, A.T. and M.N. Fienen. 2022. Modflow-setup: Robust automation of groundwater model con-  
636 struction. *Frontiers in Earth Science* 10: 903965, <https://doi.org/10.3389/feart.2022.903965>.
- 637 Lien, J.M., G. Liu, and C.D. Langevin. 2014. GRIDGEN Version 1.0: A computer program for  
638 generating unstructured finite-volume grids. U.S. Geological Survey Open-File Report 2014–1109,  
639 26 p. <https://doi.org/10.3133/ofr20141109>.
- 640 Mancewicz, L.K., A. Mayer, C.D. Langevin, and J. Gulley. 2022. Improved method for simulating  
641 groundwater inundation using the MODFLOW 6 Lake Transport Package. *Groundwater*, <https://doi.org/10.1111/gwat.13254>.
- 643 Mehl, S.W. and M.C. Hill. 2006. MODFLOW-2005, the US Geological Survey modular ground-  
644 water model-documentation of shared node local grid refinement (LGR) and the boundary flow and  
645 head (BFH) package. U.S. Geological Survey Techniques and Methods, book 6, chap. A12, 78 p.  
646 <https://doi.org/10.3133/tm6A12>.
- 647 Mehl, S.W. and M.C. Hill. 2013. MODFLOW-LGR—Documentation of ghost node local grid refine-  
648 ment (LGR2) for multiple areas and the boundary flow and head (BFH2) package. U.S. Geological  
649 Survey Techniques and Methods, book 6, chap. A44, 43 p. <https://doi.org/10.3133/tm6A44>.
- 650 Morway, E.D., C.D. Langevin, and J.D. Hughes. 2021. Use of the MODFLOW 6 water mover package  
651 to represent natural and managed hydrologic connections. *Groundwater* 59, no. 6: 913–924, <https://doi.org/10.1111/gwat.13117>.

- 653 Panday, S., C.D. Langevin, R.G. Niswonger, M. Ibaraki, and J.D. Hughes. 2013. MODFLOW-USG  
654 version 1—An unstructured grid version of MODFLOW for simulating groundwater flow and tightly  
655 coupled processes using a control volume finite-difference formulation. U.S. Geological Survey Tech-  
656 niques and Methods, book 6, chap. A45, 66 p.
- 657 Pollock, D.W.. 2014. Personal communication. Reston, VA.
- 658 Provost, A.M., C.D. Langevin, and J.D. Hughes. 2017. Documentation for the “XT3D” Option in  
659 the Node Property Flow (NPF) Package of MODFLOW 6. U.S. Geological Survey Techniques and  
660 Methods, book 6, chap. A56, 46 p. <https://doi.org/10.3133/tm6A56>.
- 661 Rew, R. and G. Davis. 1990. NetCDF: an interface for scientific data access. *IEEE computer graphics  
and applications* 10, no. 4: 76–82.
- 663 Rew, R., E. Hartnett, J. Caron, et al.. 2006. NetCDF-4: Software implementing an enhanced data  
664 model for the geosciences. In *22nd International Conference on Interactive Information Processing  
Systems for Meteorology, Oceanograph, and Hydrology*, Volume 6.
- 666 Rossetto, R., G. De Filippis, I. Borsi, L. Foglia, M. Cannata, R. Criollo, and E. Vázquez-Suñé. 2018.  
667 Integrating free and open source tools and distributed modelling codes in GIS environment for  
668 data-based groundwater management. *Environmental Modelling & Software* 107: 210–230, <https://doi.org/10.1016/j.envsoft.2018.06.007>.
- 670 Schroeder, W., K. Martin, and B. Lorensen. 2006. *The Visualization Toolkit* (4th ed.). Kitware.
- 671 Shewchuk, J.R.. 1996. Triangle: Engineering a 2D Quality Mesh Generator and Delaunay Trian-  
672 gulator. In *Applied Computational Geometry, Towards Geometric Engineering, FCRC'96 Work-  
673 shop, WACG'96, Philadelphia, PA, USA, May 27-28, 1996, Selected Papers*, pp. 203–222. <https://doi.org/10.1007/BFb0014497>.
- 675 Starn, J.J. and K. Belitz. 2018. Regionalization of Groundwater Residence Time Using Metamodeling.  
676 *Water Resources Research* 54, no. 9: 6357–6373, <https://doi.org/10.1029/2017WR021531>.
- 677 Sun, A.Y.. 2018. Discovering State-Parameter Mappings in Subsurface Models Using Generative Ad-  
678 versarial Networks. *Geophysical Research Letters* 45, no. 20: 11,137–11,146, <https://doi.org/10.1029/2018GL080404>.
- 680 U.S. Geological Survey. 2018. GWWebFlow—a browser-based groundwater model viewer. <https://webapps.usgs.gov/gwwebflow/>.
- 682 van Engelen, J., G.H. Oude Essink, H. Kooi, and M.F. Bierkens. 2018. On the origins of hypersaline  
683 groundwater in the Nile Delta aquifer. *Journal of Hydrology* 560: 301–317, <https://doi.org/10.1016/j.jhydrol.2018.03.029>.
- 685 Vilhelmsen, T.N., S. Christensen, and S.W. Mehl. 2012. Evaluation of MODFLOW-LGR in connection  
686 with a synthetic regional-scale model. *Groundwater* 50, no. 1: 118–132.
- 687 Virtanen, P., R. Gommers, T.E. Oliphant, M. Haberland, T. Reddy, D. Cournapeau, E. Burovski,  
688 P. Peterson, W. Weckesser, J. Bright, S.J. van der Walt, M. Brett, J. Wilson, K.J. Millman,  
689 N. Mayorov, A.R.J. Nelson, E. Jones, R. Kern, E. Larson, C.J. Carey, İ. Polat, Y. Feng, E.W.  
690 Moore, J. VanderPlas, D. Laxalde, J. Perktold, R. Cimrman, I. Henriksen, E.A. Quintero, C.R.  
691 Harris, A.M. Archibald, A.H. Ribeiro, F. Pedregosa, P. van Mulbregt, and SciPy 1.0 Contributors.  
692 2020. SciPy 1.0: Fundamental Algorithms for Scientific Computing in Python. *Nature Methods* 17:  
693 261–272, <https://doi.org/10.1038/s41592-019-0686-2>.

- 694 White, J.T.. 2018. A model-independent iterative ensemble smoother for efficient history-matching  
695 and uncertainty quantification in very high dimensions. *Environmental Modelling & Software* 109:  
696 191–201, <https://doi.org/10.1016/j.envsoft.2018.06.009>.
- 697 Zhou, Z. and D.M. Tartakovsky. 2021. Markov chain Monte Carlo with neural network surrogates:  
698 application to contaminant source identification. *Stochastic Environmental Research and Risk As-*  
699 *sessment* 35, no. 10: 639–651, <https://doi.org/10.1007/s00477-020-01888-9>.
- 700 Zipper, S.C., T. Gleeson, B. Kerr, J.K. Howard, M.M. Rohde, J. Carah, and J. Zimmerman. 2019.  
701 Rapid and Accurate Estimates of Streamflow Depletion Caused by Groundwater Pumping Using  
702 Analytical Depletion Functions. *Water Resources Research* 55, no. 7: 5807–5829, <https://doi.org/10.1029/2018WR024403>.